NUMERICAL SIMULATIONS OF STRATIFIED TURBULENT FLOW WITH USAGE OF HIGH ORDER SCHEMES WENO AND ILES

Aleš Jirk[1] and Josef Brechler[1]

[1]Charles University, Faculty of Mathematics and Physics, Department of Meteorology and Environment Protection, V Holesovickach 2, 180 00 Prague, Czech Republic

Abstract: The contribution discusses fully developed turbulent flow in complex geometry with respect to temperature stratification of the fluid. Numerical simulations are solved for varied Reynolds and Froude numbers to ensure the different influence of turbulence and stratification. Several cases are computed, e.g. Taylor-Green vortex (TGV) and simulations of 3D street canyon as analogy of 2D Lid-driven cavity. The employed model consists of the Navier–Stokes equations with the Boussinesq approximation, the continuity equation in the form for incompressible fluid flow, and the prognostic equation for fluctuations in potential temperature. Conservative high-order methods are used to solve the system of equations. The advection terms are reconstructed using the fifth-order weighted essential non-oscillatory (WENO) scheme and temporal evolution is solved by application of the explicit total variation diminishing (TVD) Runge–Kutta scheme. Implicit large eddy simulation (ILES) is employed as the turbulent model (part of WENO scheme). Near the borders of the obstacle wall functions are used. Results of 3D street canyon show development of turbulence with respect to increase of Reynolds number. The influence of stratification ensured by Froude number is evident with mixing of turbulence. The influence of the density of mesh on numerical results is commented on. The solutions presented are found to be in good agreement with experimental and numerical results found in the literature.

Key words: *3D stratified flow, ILES, WENO scheme.*

INTRODUCTION

Flow can be divided into three areas which can be defined by the dimensionless Reynolds number. For the lowest values of this characteristic number below *1000* we can speak of laminar flow and for large values e.g. greater than about *20 000* we can speak of turbulent flow. The area between the laminar and the turbulent flow can be marked as the transition region. Fluid motion in the atmosphere has the turbulent character except special cases like a thin laminar sub layer which can occur over laminar smooth surfaces.

Flow can be described using the law of conservation of momentum and mass. A model for incompressible fluid is used in this work. The model contains nonlinear partial differential equations whose analytical solution is unknown except for special cases and therefore efforts are to find a solution using numerical methods. More sophisticated numerical methods must be used in the calculations to correctly resolve the nonlinear parts of the differential equations (turbulence). Turbulent models that need to be used in the calculations may be added as explicit numerical schemes such as the Large Eddy Simulation (LES) method, which adds the sub-grid scale model, or schemes with the implicitly included turbulent model can be used. In this work high order accuracy schemes are used with the implicit model of turbulence (ILES).

This article describes the basic 3D numerical simulation examples TGV and Lid-driven cavity. The fundamentals are observed depending on the strength of the turbulence. TGV simulation results are compared with the literature. The discrete Fourier transformation (DFT) is employed for solving the individual components of the flow.

GOVERNING SYSTEM

The equations representing the conservation laws of various quantities are used to describe fluid motion. The conservation of momentum is covered by the Navier-Stokes equations (1). These three equations are completed with the continuity relation (2). The equations are derived in (Jirk 2008) and are written in a non-dimensional form for *i=1, 2, 3*. Stratification is employed using the Boussinesq approximation, which adds an equation for perturbations in the potential temperature (3) to the system.

$$\frac{\partial v_i}{\partial t} + \frac{\partial v_i v_k}{\partial x_k} = -\frac{\partial p}{\partial x_i} + \frac{1}{\mathrm{Re}} \Delta v_i + \frac{1}{Fr} \frac{\theta'}{\overline{\theta}} \tag{1}$$

$$\frac{\partial v_i}{\partial x_i} = 0, \tag{2}$$

$$\frac{\partial \theta'}{\partial t} + v_k \frac{\partial \theta'}{\partial x_k} = -v_3 \frac{\partial \overline{\theta}}{\partial x_3}, \tag{3}$$

where v_i are the components of velocities, x_i coordinates, t time, p pressure, Θ potential temperature, Re Reynolds number and Fr Froude number.

NUMERICAL METHODS

The finite volume method is used for the spatial discretization of the governing equations (1-3) (see, for example, Ferziger, Perić 1997 or McDonough 2003). The whole system of the Navier-Stokes equations (1) and the continuity relation (2) is solved by the fractional – step method (Brown et al. 2001). This approach splits the solution of the equations into several steps. In this work the three step method has been applied.

The advection terms in (1) are reconstructed by the WENO scheme (Liu et al. 1994) that was extended from the ENO scheme (Harten et al. 1987) and (Shu, Osher 1988). A key idea in the WENO scheme is a linear combination of lower order fluxes or reconstructions to obtain a higher order approximation. Both the ENO and WENO schemes use the idea of adaptive stencils to automatically achieve high order accuracy and non-oscillatory property near discontinuities. In this work the WENO scheme of fifth-order accuracy has been employed **(**Titarev, Toro 2004). The explicit TVD Runge-Kutta scheme of third-order accuracy (Gottlieb, Shu 1998) has been used for the computation of the temporal partial derivation in (1). The semi-implicit Crank-Nicholson method (Kim et al. 2001) is applied for computing the viscous term in (1) . Near the borders of the obstacle wall functions are used. The ILES method that goes hand in hand with the WENO scheme is employed as the turbulent model. It is implicitly added by the WENO scheme as the form of LES in which the structures with large energy are resolved, while the smaller more isotropic structures are filtered out, therefore their effects need to be modeled. As the third step of the fractional-step method the pressure term in (1) is added to the system as the pressure correction (Ferziger, Perić 1997).

PRESENTATION OF RESULTS

Results are demonstrated by variables which describe the solution. In this contribution kinetic energy (4), vorticity (5) and 2D stream function (6) are computed and then depicted in figures:

$$E_k = \frac{1}{2} v_i^2, i = 1,2,3 \tag{4}$$

$$\omega = \nabla \times v, \tag{5}$$

$$v_1 = \frac{d\psi}{dx_2}, v_2 = -\frac{d\psi}{dx_1}, \tag{6}$$

E_k is kinetic energy, v velocity, ω vorticity, ψ 2D stream function and x_i coordinates.

For investigating turbulence the flow in computed area is transformed via DFT into wave space. The 3D Fourier image $X_{j,k,l}$ is defined by the equation (Burrus et al, 2009):

$$X_{j,k,l} = \sum_{m=0}^{M-1} \sum_{n=0}^{N-1} \sum_{o=0}^{O-1} x_{m,n,o} e^{-imj\,2\pi/M} e^{-ink\,2\pi/N} e^{-iol\,2\pi/O} \tag{7}$$

$x_{m,n,o}$ is a periodical sequence with period M,N,O and i is the complex number. $i = \sqrt{-1}$. The fast Fourier transformation algorithm (Cooley, Tukey 1965) for sequence $N=2^a$ (a is a natural number) is employed for the solution of equation (7).

RESULTS AND DISCUSSION

In this work the results of TGV (Taylor – Green Vortex) and Lid-driven cavity cases are shown and discussed. All results are compared with the literature and the influence of Reynolds number on behavior of kinetic energy and on the features of amplitudes of wave numbers with usage of DFT is investigated.

TGV configuration involves triple-periodic boundary conditions enforced on a cubical domain with box side length *1* using 256^3 evenly spaced computational cells. The boundary periodic conditions are used for both the velocity components and pressure. The initial conditions are written as (8):

$$v(t=0) = (\sin(2\pi x_1)\cos(2\pi x_2)\cos(2\pi x_3), -\cos(2\pi x_1)\sin(2\pi x_2)\cos(2\pi x_3), 0) \tag{8}$$

The time dependence of kinetic energy is depicted in figure 1a. The decrease of energy occurs in different characteristic dimensionless times for each Reynolds number, the fastest decrease is found for the lowest Reynolds number. The energy decrease results are in good agreement with the literature (Drikakis et al, 2006).

a) b)

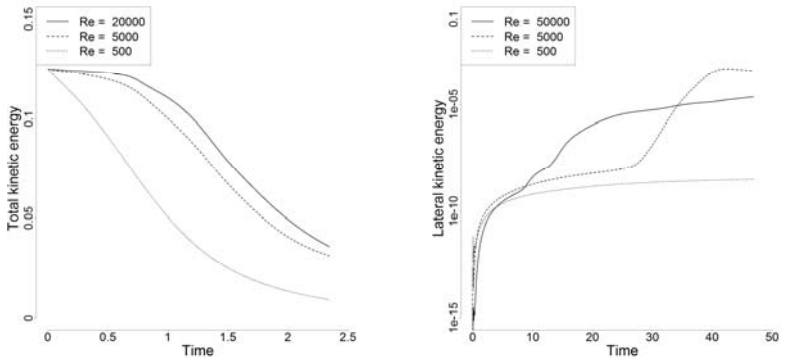

Figure 1. The dependence of kinetic energy on time with various Reynolds numbers: a) TGV, b) Lid-driven cavity

The 3D Lid – driven cavity flow is the analogy to the well-known 2D case. It is flow in the cubic domain with lateral periodic conditions and inflow, outflow and bottom walls with the solid wall condition. The x – component of the velocity is equal to *1* is taken as the top wall initial and boundary condition. Simulation was made on computation area 128^3. Reynolds numbers *500*, *5 000* and *50 000* were used during the computation to estimate the three characteristics of fluid flow –laminar, transition region and turbulent.
For Reynolds number *1 000* the coordinates of the primary and secondary vortices were determined with $\sigma = \pm 0.004$ accuracy, compared with the literature and the results are in good agreement as mentioned in table 1.

Table 1. Coordinates of primary and secondary vortices for *Re = 1000*

Vortex	This work (3D)	Jirk 2008 (2D)	Ghia et al., 1982 (2D)
Primary	(0.535; 0.565)	(0.533; 0.562)	(0.531; 0.562)
Secondary	(0.871; 0.110)	(0.868; 0.111)	(0.859; 0.109)

This verification confirmed the correct computation of the WENO scheme. Further the dependence of the Reynolds number on the behaviour of the flow inside the entire area was investigated. The influence of turbulence on the temporal development of lateral kinetic energy over 3D area was monitored as is depicted in figure 1b. It is evident that the kinetic energy dependence can be divided into 3 areas as mentioned above. The transition region between laminar and turbulent flow for Reynolds numbers about *5 000* has in the beginning the character of the laminar one and gradually becomes turbulent.
For the investigation of the flow areas DFT was used over each surface perpendicular to the axis x to find the amplitudes of the 64 wavenumbers (in fact 128 wavenumbers but they are doubled). The spatial distribution of these amplitudes with respect to the x – coordinates of the computed area is depicted in figure 2 for Reynolds numbers *500, 5 000* and *50 000* in three dimensionless times. In figure 3 the stream functions of selected wavenumbers computed from inverse DFT are shown for same Reynolds numbers as in figure 2 in one dimensionless time equal to *16*.
The behaviour of the amplitudes differs in respect to the Reynolds number. For the low Reynolds number a stable solution is established in a short time. The low wavenumbers are much more significant than the higher ones and no significant changes are visible in the wave characteristic at longer times. On the contrary for *Re 50 000* the higher wavenumbers are more significant and their spatial distribution is set up during a longer time period.

a)

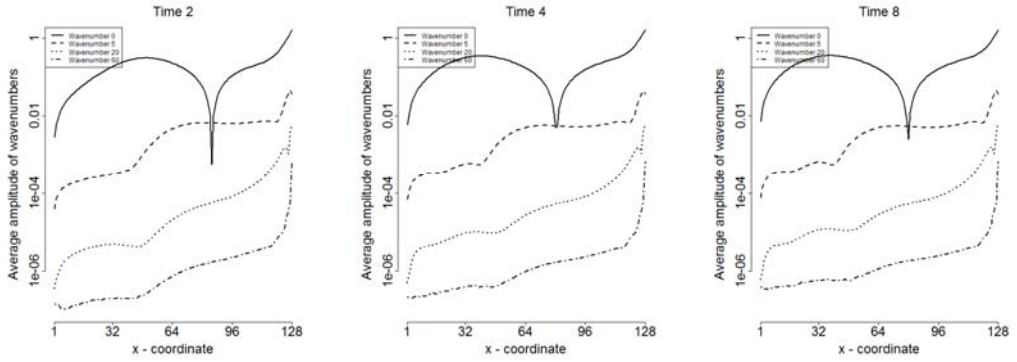

b)

c)

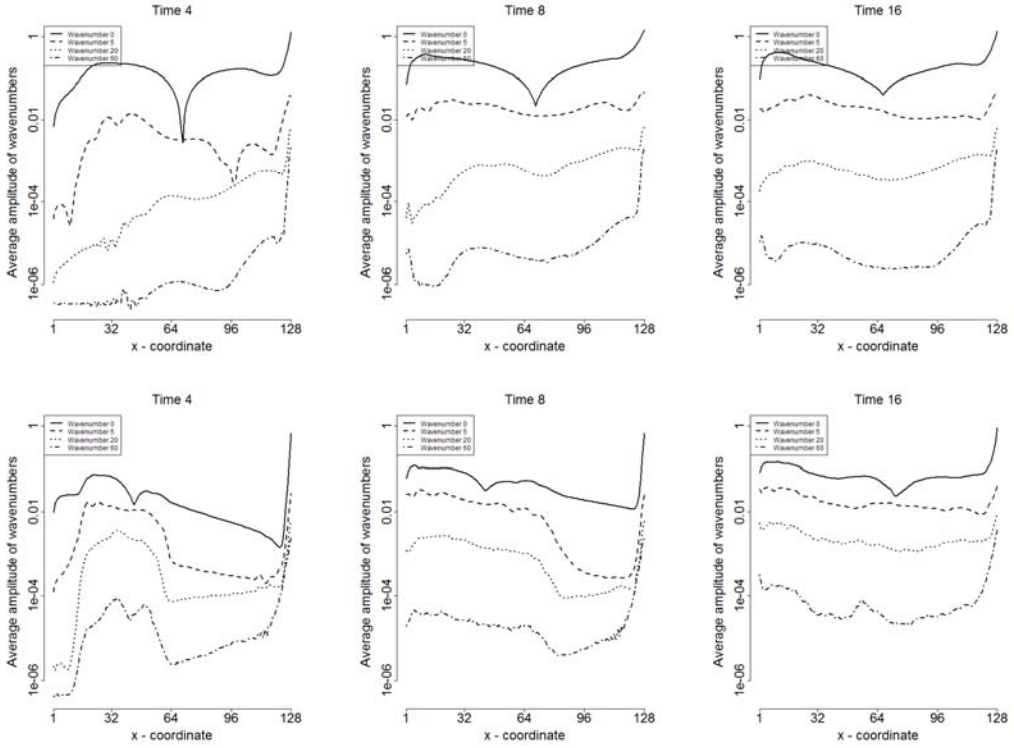

Figure 2. Dependence of wavenumber amplitude of x component of velocity on x – coordinates in time:
a) *Re = 500*, b) *Re = 5000*, c) *Re = 50 000*

The graphic representation of the stream function divided for the lowest wavenumbers and the remainder shows the distribution of the main flow for wavenumbers 0 – 3 and additional smaller vortices for wavenumbers 4 – 63. The main stream is located in the top row, the bottom one shows the remaining wavenumbers and images oscillation with the higher wavenumbers. The higher wavenumbers occur more often for higher Reynolds numbers as is evident from both figures 2 and 3.

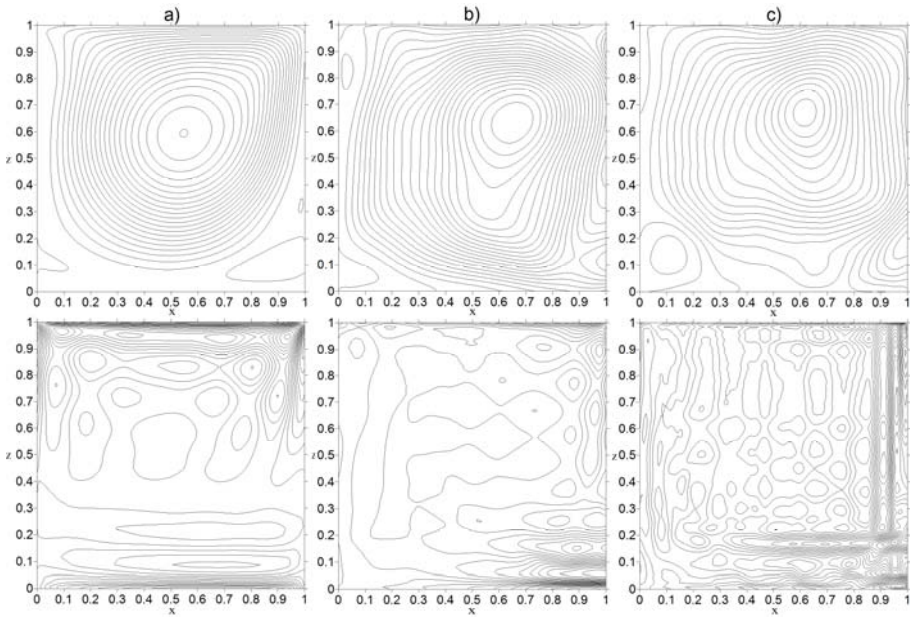

Figure 3. Lid- driven cavity case; x-z cross-section; Stream Function, top main stream, bottom secondary stream:
a) Re = 500, b) Re = 5000, c) Re = 50 000

The Lid – driven cavity case was computed also with the usage of stratification. The results for the variety of Froude numbers were compared with (Iwatsu et al., 1992) and they are in good agreement. The result for *Re 400* and the Froude number *Fr = 0.1* is shown in figure 4. The strength of stable stratification means that the primary vortex is largely confined to the upper part of the cavity. The influence of the upper boundary velocity (primary vortex) extends over a smaller area within the cavity because the stable stratification acts to suppress vertical motion. Vertical exchange is strongly suppressed, especially in the lower part where it becomes chaotic.

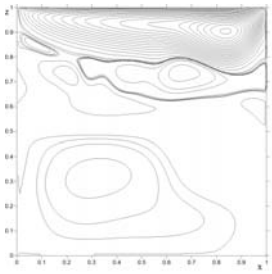

Figure 4. Stratified Lid- driven cavity case, x-z cross-section; Stream Function, Re = 400, Fr = 0.1

CONCLUSION

Higher accuracy schemes were used in this contribution for the simulation of the turbulent 3D cases TGV and Lid driven cavity. All the results are in good agreement with the literature. It confirms the usage of the WENO scheme for advection term reconstruction and handling turbulence as the ILES model. In both cases we presented the development of laminar and turbulent flow. The wavenumber analysis was made with the usage of DFT. The flow can be split into main flow and fluctuations which can be described by the wavenumbers. With the inverse DFT we can compute the divided flow. The results show the main flow and small vortexes which are involved in the higher wavenumber flow. The higher wavenumbers have higher influence for the turbulent flow than for the laminar one. The time dependence of the kinetic energy divides the flow into three characteristic regions. The stratification influence was computed for the Lid-driven cavity case for low Reynolds numbers and various Froude numbers. Stable stratifications supress vertical motion and the primary vortexes are shifted to the top boundary.

REFERENCES

Brown, D. L., Cortez, R. and Minion, L. M., 2001. Accurate Projection Methods for the Incompressible Navier-Stokes Equations. Journal of Computational Physics 168, 464-499.

Burrus,C.S., Frigo,M., Johnson,S.G.,Pueschel, M., Selesnick,I., 2009, Fast Fourier Transforms, Rice University, Houston, Texas, http://cnx.org/content/col10550/latest

J. W. Cooley and J. W. Tukey. An algorithm for the machine calculation of complex Fourier series. Math. Computat., 19:2978211;301, 1965.

Drikakis D., Fureby Ch., Grinstein F. F., Hahn M. and Youngs D., LES of Transition to Turbulence in the Taylor Green Vortex, book Direct and Large-Eddy Simulation VI, 2006, Springer

Ferziger, J. H. and Peric, M., 1997. Computational Methods for Fluid Dynamics. Springer Verlag, Berlin.

Ghia, U., Ghia, K. N. and Shin, C. T., 1982. High-Resolutions for Incompressible Flow Using the Navier-Stokes Equations and a Multigrid Metod. Journal of Computational Physics 48, 387-411.

Gottlieb,S.,Shu, Ch.W., 1998, Total variation diminishing Runge-Kutta schemes, Mathematics of Computation 67 (221), 73-85

Harten, A., Enquist, B., Osher, S. a Chakravarthy, S.R., 1987. Uniformly High Order Accurate Essentially Non-Oscillatory Schemes, III. Journal of Computational Physics 71, 231-303.

Iwatsu, R., Hyun, J., M. and Kuwahara, K., 1992. Mixed convection in a driven cavity with a stable vertical temperature gradient. Int. Journal Heat Mass Transfer. Vol 36, No.6.

Jirk, A., 2008. Thermally stratified atmospheric flow modelling. Diploma thesis. Dept of Meteorology and Env. Protect., MFF UK Prague (in Czech).

Kim, J., Kim, D. and Choi, H., 2001. An immersed-Boundary Finite-Volume Metod for Simulations of Flow in Complex Geometry. Journal of Computational Physics 171, 132-150.

Liu, X. D., Osher, S. and Chan T., 1994. Weighted Essentially Non-Oscillatory Schemes. Journal of Computational Physics 115, 200-212.

Shu, CH. W. a Osher, S., 1988. Efficient Implementation of Essentially Non-Oscillatory Shock-Capturing Schemes. Journal of Computational Physics 77, 439-471

Titarev, V. A. a Toro, E. F., 2004. Finite-Volume WENO Schemes for Three-Dimensional Conservation Laws. Journal of Computational Physics 201, 238-260